Available online at www.sciencedirect.com
SCIENCE DIRECT®
Journal of Sound and Vibration 286 (2005) 615–636
JOURNAL OF SOUND AND VIBRATION
www.elsevier.com/locate/jsvi

Passive–active vibration isolation systems to produce zero or infinite dynamic modulus: theoretical and conceptual design strategies

J.T. Xing*, Y.P. Xiong, W.G. Price

The School of Engineering Sciences, Ship Science, University of Southampton, Highfield, Southampton SO17 1BJ, England, UK

Received 8 August 2003; received in revised form 11 October 2004; accepted 13 October 2004
Available online 5 January 2005

Abstract

The application of mechanical springs connected in parallel and/or in series with active springs can produce dynamical systems characterised by infinite or zero value stiffness. This mathematical model is extended to more general cases by examining the dynamic modulus associated with damping, stiffness and mass effects. This produces a theoretical basis on which to design an isolation system with infinite or zero dynamic modulus, such that stiffness and damping may have infinite or zero values. Several theoretical designs using a mixture of passive and active systems connected in parallel and/or in series are proposed to overcome limitations of feedback gain experienced in practice to achieve an infinite or zero dynamic modulus. It is shown that such systems can be developed to reduce the weight supported by active actuators as demonstrated, for example, by examining suspension systems of very low natural frequency or with a very large supporting stiffness or with a viscous damper or a self-excited vibration oscillator. A more general system is created by combining these individual systems allowing adjustment of the supporting stiffness and damping using both displacement and velocity feedback controls. Frequency response curves show the effects of active feedback control on the dynamical behaviour of these systems. The theoretical design strategies presented can be applied to design feasible hybrid vibration control systems displaying increased control performance.

*Corresponding author. Tel.: +44 23 8059 6549; fax: +44 23 8059 3299.
E-mail address: j.t.xing@ship.soton.ac.uk (J.T. Xing).

0022-460X/$ - see front matter © 2004 Elsevier Ltd. All rights reserved.
doi:10.1016/j.jsv.2004.10.018

1. Introduction

The demand for higher performance vibration suspension systems has increased in many scientific and industrial fields such as semiconductor manufacturing, engine mounts for automotives and support systems with very low supporting frequencies as required in vibration tests of large aircraft stationed on the ground. In general, there are two kinds of disturbances to be isolated by suspension systems. One is vibration transmitted from the ground to the equipment standing on the ground and the other is vibration, produced by machines, transmitting to the ground. As discussed by Harris and Crede [1] and Thomson [2], softer suspension systems are required to isolate the former vibration disturbance whereas harder suspension systems are better to suppress the latter. Both kinds of suspension systems, with lower or higher dynamic stiffness, are needed in practical designs. However, for some cases, they cannot be realised because the performance of conventional passive-type vibration isolation systems is limited. To improve performance, various types of active actuators have been introduced into these isolation systems. In a recent comprehensive, critical review of engine mounts for automotive applications, Jazar and Golnaraghi [3] provide the history (together with 115 references) and development of passive and active isolation theories and their practical design. To isolate precision payloads from spacecraft borne disturbances, Cobb et al. [4] present the design and performance of a vibration isolation and suppression system using a novel hybrid actuator concept to provide both passive isolation and active damping. The theoretical schematic diagram of this isolation system consists of three parallel-connected components: a static stiffness K_a, an actuator that is a voice coil motor providing an active force relating to the motion velocity, and a fluid damper C_a connected in series with a volumetric stiffness K_b. This vibration isolation suspension system was designed to have a low suspension frequency in the range of 2–5 Hz. They describe details of real designs involving sensors, control system architecture, etc. and present information derived from performance tests. Platus et al. [5] proposed a vibration isolation system using a conventional spring connected in parallel with a fully passive, negative-stiffness-mechanism to produce a reduced value of the supporting stiffness. Mizuno [6] proposed to use a mechanical spring connected in series to an electro-magnetic active spring (i.e. a zero-power magnetic suspension) to obtain a very high value of the supporting stiffness, which was further studied and successfully demonstrated by experiments [6–8]. Kwak et al. [9] presented the development of a passive–active vibration absorber using piezoelectric actuators, in which combinations of passive and active systems are adopted in parallel and series. They discussed the limitations of the piezoelectric actuator to support heavy equipment.

Fuller et al. [10] describe active feedback controls using displacement, velocity and acceleration parameters to modify the effective mass, damping and stiffness of a system. However, the use of parallel or series connections of mechanical springs with an active spring to produce a lower [5] or higher [6] supporting stiffness has not been investigated to general cases involving all feedback possibilities. This paper investigates whether such systems can be constructed to produce an infinite or zero damping and whether they can be implemented. In practical designs of isolation or suspension systems [5–6], realisable displacement feedback gains are limited by insufficient generation of negative stiffness to balance the large stiffness mechanical springs and hence, to derive the required isolation performance. For example, in a vibration resonance test of a grounded aircraft, to reduce the effect of the suspension system on the natural frequencies of the

aircraft, the suspension frequency is required to be less than one third of the first natural frequency of the aircraft [11]. For a large aircraft, such as a Boeing 707, its first natural frequency is about 1 Hz, and therefore, the suspension frequency required is approximately 0.3 Hz. To design such a supporting system is difficult, because to support the aircraft, a sufficiently strong spring is necessary which contributes to a higher suspension frequency. If we simply adopt a controller in parallel with a mechanical spring to produce a lower supporting frequency [5], a very large feedback gain is required. However, such large feedback gains may also be unachievable in practical active feedback devices yet there remains the requirement to design an active control system with limited feedback gain to provide the required suspension performance.

This paper discusses the development of a generalised theory to incorporate not just stiffness but also the dynamic modulus [1] of the system. That is, a passive isolator model to include mass, stiffness and damping characteristics; an active controller taking into account displacement, velocity and acceleration feedbacks and to investigate whether it is possible to produce designs with infinite or zero damping. To illustrate the latter and to overcome the limitations of practical active feedback control systems, several theoretical mixed arrangements of parallel and series components are proposed.

2. Fundamental theory

Based on the studies of Platus et al. [5] and Mizuno [6], we develop a generalised model accounting for dynamic modulus [1] arising from stiffness, damping and mass effects. This provides a basis on which to investigate an isolation system to produce infinite or zero damping. As shown in Fig. 1, a typical vibration isolation unit consists of a spring of stiffness coefficient k, a damper of viscous coefficient c and a lumped mass m. The relation between the input force $f = F\mathrm{e}^{\mathrm{j}\omega t}$ and the output displacement $u = U\mathrm{e}^{\mathrm{j}\omega t}$ is represented as

$$f = m\ddot{u} + c\dot{u} + ku = (k + \mathrm{j}\omega c - m\omega^2)u = Du, \tag{1}$$

where $D = k + \mathrm{j}\omega c - m\omega^2$ denotes the dynamic modulus of the isolator.

Let us examine the generalised single-channel feedback control system shown in Fig. 2. This idealised system produces a secondary downward force f_c having components proportional to acceleration $\ddot{u}_c$, velocity $\dot{u}_c$ and displacement u_c which represent relative values between the top and bottom of the actuator. Because the bottom is fixed, these variables describe the absolute

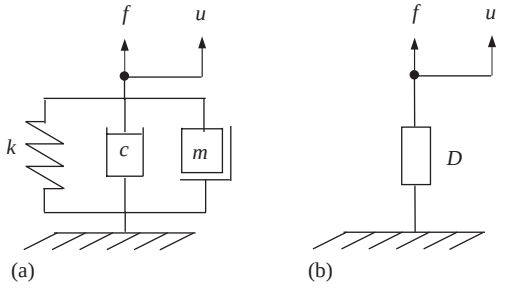

Fig. 1. (a) A generalised passive vibration isolator. (b) The equivalent system with dynamic modulus D.

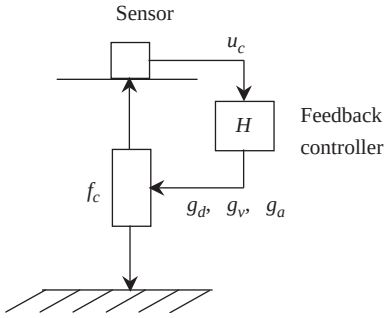

Fig. 2. A single-channel feedback control system.

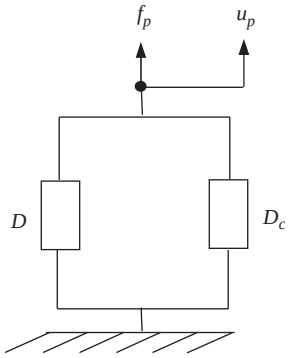

Fig. 3. An isolator and feedback controller connected in parallel.

quantities at the top of the actuator and the force is given as

$$f_c = g_a\ddot{u}_c + g_v\dot{u}_c + g_d u_c = (g_d + \mathrm{j}\omega g_v - g_a\omega^2)u_c = D_c u_c, \tag{1'}$$

where g_a, g_v and g_d represent the feedback gain constants and $D_c = g_d + \mathrm{j}\omega g_v - g_a\omega^2$ is the dynamic modulus of the feedback controller. Therefore, the displacement, velocity and acceleration feedback controls can modify the stiffness, damping and inertia characteristics of the system as described by Fuller et al. [10].

2.1. Parallel connection of an isolator and a feedback controller

When an isolator and a feedback controller are connected in parallel as shown in Fig. 3, the total dynamic modulus D_p is given by

$$D_p = D + D_c = (k + g_d) + \mathrm{j}\omega(c + g_v) - (m + g_a)\omega^2. \tag{2}$$

An investigation of this equation allows a vibration suspension system with zero dynamic modulus to be defined. Namely, in theory,

$$D_p = D + D_c = 0, \tag{3}$$

because the feedback gains g_a, g_v and g_d can be adjusted from negative to positive values. For example, if

$$k + g_d = 0, \quad c + g_v = 0, \quad m + g_a = 0, \tag{4}$$

then Eq. (3) is satisfied provided that parameters m, c and k of this passive isolator are accurately known.

If only a spring of stiffness k and a displacement feedback control gain g_d are considered, Eq. (2) reduces to the special case investigated by Platus et al. [5], where g_d corresponds to a fully passive, negative stiffness mechanism.

2.2. An isolator and feedback controller connected in series

When an isolator and a feedback controller are connected in series as shown in Fig. 4, the total dynamic modulus D_s is given by

$$D_s = \frac{DD_c}{D + D_c} = \frac{(k + \mathrm{j}\omega c - m\omega^2)(g_d + \mathrm{j}\omega g_v - g_a\omega^2)}{(k + g_d) + \mathrm{j}\omega(c + g_v) - (m + g_a)\omega^2}. \tag{5}$$

This equation allows a vibration suspension system with infinite dynamic modulus to be defined. Namely,

$$|D_s| = \left|\frac{DD_c}{D + D_c}\right| = \infty \tag{6}$$

if the condition

$$D + D_c = 0 \tag{7}$$

is satisfied exactly by adjusting the feedback gains g_d, g_v, g_a.

If only a spring of stiffness k and a displacement feedback control gain g_d are considered, Eq. (5) reduces to the special case investigated by Mizuno [6], where the gain g_d corresponds to the electro-magnetic spring producing a zero-power magnetic suspension.

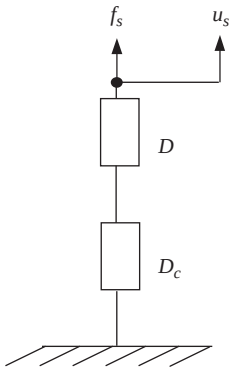

Fig. 4. An isolator and feedback controller connected in series.

3. Theoretical design strategies

The generalised principles of isolation systems with a zero or infinite dynamic modulus described previously can be applied to vibration isolation systems. To illustrate this, several theoretical design strategies are now discussed.

3.1. A suspension system with very low suspension frequency

For some engineering cases, a very low suspension frequency is required. For example, the supporting system used in resonance experiments of full-scale, grounded aircraft [11]. Fig. 5 illustrates a schematic representation of this suspension system, where M denotes the mass of the aircraft, k and c denote the stiffness and damping coefficients of the mechanical device supporting the static weight of the aircraft. The feedback control system provides a dynamic force $f_c = g_d u$ proportional to the displacement. A direct current signal isolator is used so that the feedback system produces only alternating forces acting on the mass. Therefore, the feed back system does not affect the static stiffness of the supporting system.

The equilibrium equation describing this system at its static equilibrium position is given by

$$Mg = k\delta, \tag{8}$$

where g and δ represent the acceleration of gravity and the static compression deformation of the mechanical spring, respectively. The dynamic equilibrium equation defined about the static equilibrium position is represented by

$$M\ddot{u} + c\dot{u} + (k + g_d)u = 0, \tag{9}$$

where u denotes the dynamic displacement of the mass translated from its static equilibrium position. The frequency of the supporting system is now given by

$$\Omega = \sqrt{\frac{k + g_d}{M}}, \tag{10}$$

which can produce the required supporting frequency by choosing a negative gain g_d.

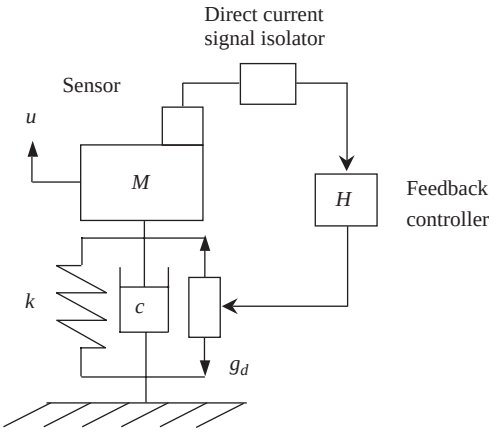

Fig. 5. A suspension system with a very low suspension frequency.

The characteristic equation of Eq. (9) is

$$\lambda^2 + 2\zeta\Omega\lambda + \Omega^2 = 0, \tag{11}$$

where $\zeta = c/2M\Omega$ represents a non-dimensional damping coefficient. To check the stability of the solutions of an ordinary differential equation with constant coefficients, necessary and sufficient conditions are established based on the Routh–Hurwitz Criterion (see, for example, [10]). For a second order system, this criterion reduces to the requirement that all the coefficients of the characteristic equation have the same sign. In fact, the eigenvalues of Eq. (11) can be written in the form

$$\lambda_{1,2} = -\zeta\Omega \pm \mathrm{j}\Omega\sqrt{1-\zeta^2}, \quad \zeta < 1, \tag{12}$$

which have negative real parts, as required for stability. For a practical mechanical supporting system, the damping coefficient c denotes the material internal damping or the damping of the moving parts of the system, which is a positive value satisfying the condition $\zeta < 1$. Therefore, a suitable negative displacement feedback gain g_d is chosen by satisfying the condition

$$-k < g_d < 0, \tag{13}$$

which produces a stable suspension system with a sufficiently low supporting frequency as given by Eq. (10).

For the system shown in Fig. 5, a mechanical spring and a negative active spring connected in parallel are used as discussed by Platus [5]. However, as described previously, to isolate any direct current signals, such as signals produced by static deflections caused by the weight of the aircraft, a direct current signal isolator is introduced. Therefore, the active feedback system can only be effective for dynamic motions excited by harmonic exciting forces used in the test. As a result, the dynamic stiffness of the supporting system around its static equilibrium position is reduced but the static stiffness of the system supporting the large weight of the aircraft remains unchanged.

For a static spring of stiffness k of moderate value such that an active feedback actuator provides a comparable feedback gain g_d, as illustrated in Eq. (10), the system shown in Fig. 5 is applicable for use as a practical design. However, if the static stiffness k is very large, i.e. to support a large aircraft, a conventional feedback controller is unable to produce a sufficiently large feedback gain g_d, and the system shown in Fig. 5, using the idea developed in [5], is not practical. Fig. 6 illustrates a modified system able to overcome this limitation. Namely, in this design, a spring of small stiffness k_1 is connected in series with an active displacement feedback controller. It is shown that two possible arrangements of the actuator and the spring k_1 produce the same dynamic characteristics of the supporting system. For example, Fig. 6(a) shows the spring k_1 connected to the ground and two sensors arranged to produce a feedback force proportional to the displacement difference $u - u_1$, which is the relative displacement at both ends of the actuator. Fig. 6(b) shows the spring k_1 connected to the mass M and the actuator now connected to the ground and only one sensor measures the top displacement of the actuator to produce the required feedback force. The static equilibrium equation of these systems is described by Eq. (8), but the dynamic equation changes to

$$M\ddot{u} + c\dot{u} + \left(k + \frac{k_1 g_d}{k_1 + g_d}\right)u = 0, \tag{14}$$

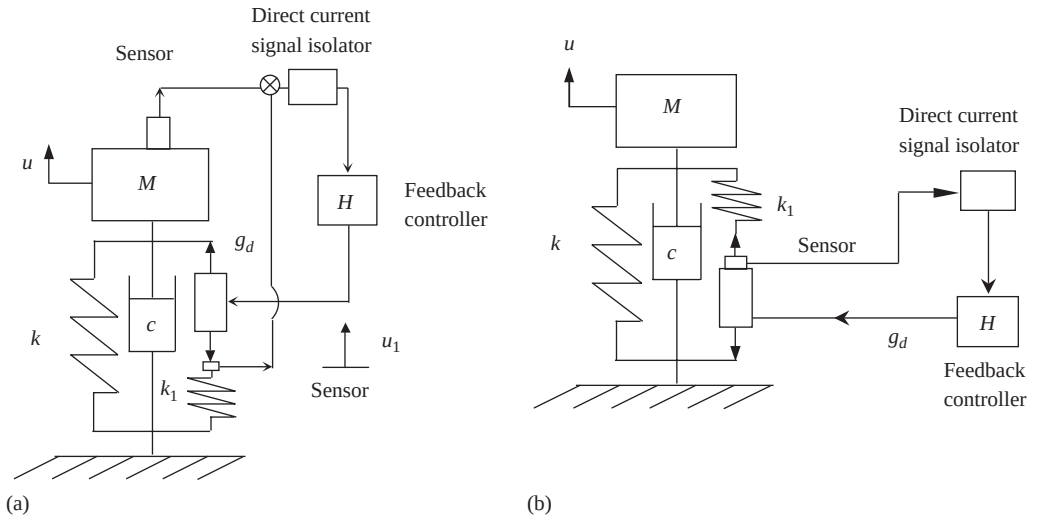

Fig. 6. Proposed suspension systems with a very low suspension frequency using a soft spring k_1 connected in series to a feedback controller to overcome practical feedback gains limitations.

which produces the suspension frequency

$$\Omega = \sqrt{\frac{k + (k_1 g_d)/k_1 + g_d}{M}} = \sqrt{\frac{k - (k_1|g_d|)/k_1 - |g_d|}{M}}. \tag{15}$$

A suitably chosen negative feedback gain g_d satisfying the condition

$$-\frac{kk_1}{k + k_1} < g_d < 0 \tag{16}$$

allows a reduced frequency to be achieved as indicated by Eq. (15).

It is noted that there is a need to distinguish between the static stiffness k in Eq. (8) and the dynamic stiffness $k - (k_1|g_d|)/k_1 - |g_d|$ in Eqs. (14) and (15). As described previously, due to the *direct current signal isolator*, the large value static stiffness k supporting the static weight M is not affected by the feedback control. In the region of the static equilibrium position of the whole system, the dynamic stiffness is adjusted to produce a supporting suspension system of very low frequency. The proposed system forms the basis on which to design successfully a supporting system with large static stiffness and very low dynamic stiffness used in full-scale vibration tests of grounded aircraft [11].

3.2. A suspension system with a very high value of suspension stiffness

To design a fixed mechanical supporting structure of infinite stiffness for dynamic experiments is not always easy. For example, a well-designed structure, which can be assumed to have a rigid characteristic in the low frequency range, may become a very soft support in the high-frequency range. As studied by Mizuno [6], a mechanical spring connected in series to an active negative

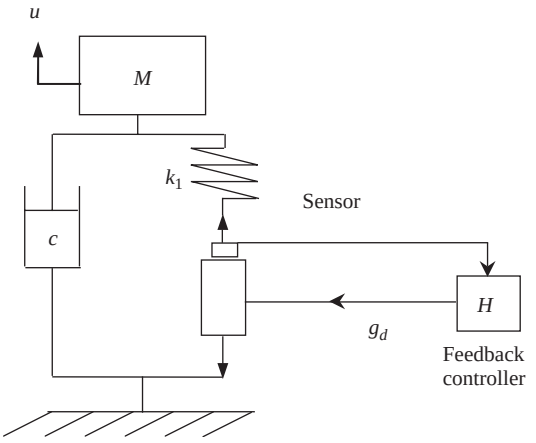

Fig. 7. A suspension system with a very high suspension stiffness.

spring produces a suspension system with very high suspension stiffness. This system is constructed by deleting the supporting spring of stiffness k and the direct current signal isolator shown in Fig. 6. For example, Fig. 7 shows a system derived from Fig. 6(b). The dynamic equilibrium equation of this system is

$$M(\ddot{u}+g)+c\dot{u}+\frac{k_1 g_d}{k_1+g_d}(u-\delta)=0, \tag{17}$$

where δ represents the static compression deformation of the supporting system, g is the acceleration of gravity and u denotes the upward dynamic displacement of the system from the static equilibrium position. A suitably chosen feedback gain g_d satisfying the condition

$$g_d \leqslant -k_1 \tag{18}$$

provides a suspension system with very high supporting stiffness and support frequency

$$\Omega=\sqrt{\frac{k_1 g_d}{M(k_1+g_d)}}=\sqrt{\frac{k_1|g_d|}{M(|g_d|-k_1)}}. \tag{19}$$

This system is also stable because the eigenvalues of its characteristic equation have negative real parts. Mizuno et al. [6–8] investigated this kind of magnetic suspension system and performed *practical experiments* to confirm the design.

As discussed by Kwak et al. [9], a limitation of the system shown in Fig. 7 arises when the actuator supports heavy equipment. To overcome this problem, Fig. 8 shows a system constructed of a mixture of parallel and series suspension systems. Here a strong mechanical spring k is introduced to support part of the weight M, which is fully supported by the active actuator as illustrated in Fig. 7. For this system, condition (18) satisfied by the feedback gain g_d remains unchanged. However, the supporting stiffness is now $k+(k_1|g_d|)/+|g_d|-k_1$ with a

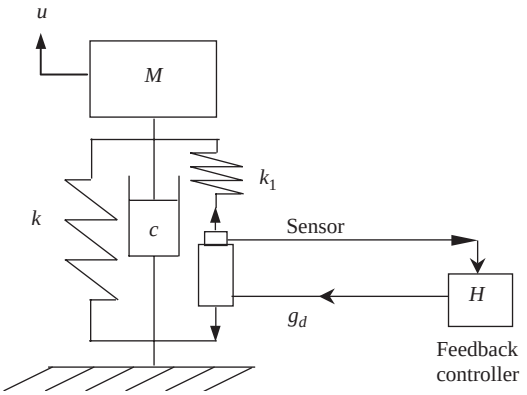

Fig. 8. A proposed suspension system with a strong mechanical spring k connected in parallel with the isolator shown in Fig. 7 to support part of the weight carried by the active actuator.

corresponding support frequency

$$\Omega = \sqrt{\left(k + \frac{k_1|g_d|}{|g_d| - k_1}\right)/M}. \tag{20}$$

3.3. A suspension system with a very high damping value

A successful vibration isolation system requires high damping to dissipate vibration energy. As shown in Fig. 3 and Eq. (2), an active damper connected in parallel with a passive damper increases the damping of the isolation system. However, in practical designs, very high active damping devices have limitations. To overcome this difficulty, Fig. 9 illustrates an active damper connected in series with a passive damper of value c_1. The dynamic equation of this system, relative to its static equilibrium position, is represented as

$$M\ddot{u} + \left(c + \frac{c_1 g_v}{c_1 + g_v}\right)\dot{u} + ku = 0, \tag{21}$$

which produces a very high active damping value when a negative velocity feedback gain g_v is chosen to satisfy the condition

$$g_v \leqslant -c_1. \tag{22}$$

3.4. A self-exited oscillator with zero damping

If the velocity feedback gain associated with the proposed system illustrated in Fig. 9 satisfies the condition

$$c + \frac{c_1 g_v}{c_1 + g_v} = 0 \quad \text{or} \quad g_v = -\frac{cc_1}{c + c_1}, \tag{23}$$

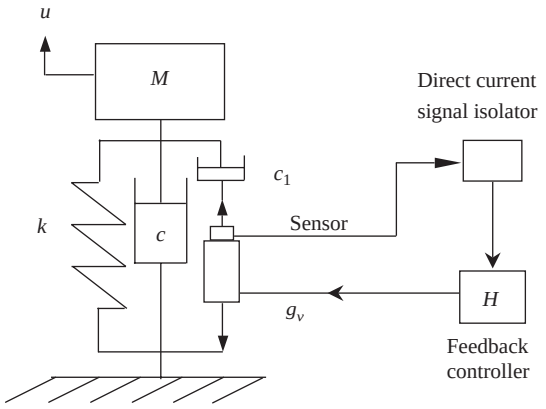

Fig. 9. A suspension system with high damping using velocity feedback control.

the damping of the system is zero and generates a self-exiting mechanical oscillator device with zero damping. This active control system complements the energy dissipated by the physical damping in the system and the initial oscillation does not decay. This principle is widely used in electrical devices [12]. The system presented in Fig. 9 exercises the concept of an active damper connected in series with a passive damper c_1, and uses a finite active velocity feedback gain of value approximately equal to c_1 to counteract the large passive damping c. To satisfy the stability requirement, the feedback gain g_v obeys the inequality

$$-\frac{cc_1}{c+c_1} < g_v < 0. \tag{24}$$

Therefore, a negative feedback gain g_v with an absolute value a little larger than $cc_1/(c+c_1)$ needs to be chosen.

3.5. A suspension system with adjustable supporting stiffness and damping

A combination of the isolation systems shown in Figs. 6 and 9 provides a supporting system, which allows adjustment of the supporting stiffness and damping using both displacement and velocity feedback controls. Fig. 10 shows the arrangement of this supporting system. The dynamic equation of the system is given by

$$M\ddot{u} + \left(c + \frac{c_1 g_v}{c_1 + g_v}\right)\dot{u} + \left(k + \frac{k_1 g_d}{k_1 + g_d}\right)u = 0, \tag{25}$$

which provides a dynamic supporting stiffness

$$\tilde{k} = k + \frac{k_1 g_d}{k_1 + g_d} = \begin{cases} \text{for high stiffness,} & g_d \leqslant -k_1, \\ \text{for low stiffness,} & -\frac{kk_1}{k+k_1} < g_d < 0 \end{cases} \tag{26}$$

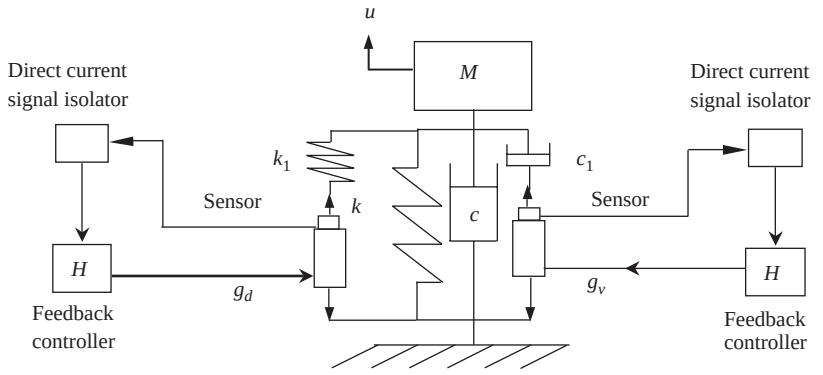

Fig. 10. A suspension system constructed by combining the systems shown in Figs. 6 and 9 to produce prescribed supporting stiffness and damping values using both displacement and velocity feedback controls.

and damping

$$\tilde{c} = c + \frac{c_1 g_v}{c_1 + g_v} = \begin{cases} \text{for high damping,} & g_v \leqslant -c_1, \\ \text{for low damping,} & -\frac{cc_1}{c+c_1} < g_v < 0. \end{cases} \tag{27}$$

The suspension frequency becomes

$$\Omega = \sqrt{\left(k + \frac{k_1 g_d}{k_1 + g_d}\right)/M}. \tag{28}$$

In the resonance testing of a full-scale aircraft stationed on the ground, to reduce the influence of the supporting system's stiffness and damping on the natural characteristics of the aircraft, it is necessary for the supporting system to have very low frequency and damping values [11]. The theoretical design shown in Fig. 10 satisfies these requirements by choosing suitable feedback gains as described in Eqs. (26) and (27).

To investigate the characteristics of the frequency response of this generalised system, let us assume that the force $f = Fe^{j\omega t}$ is applied to the mass. The amplitude factor describing the displacement response of the mass is given by

$$\sigma(\bar{\omega}) = \frac{MU\omega_0^2}{F} = \frac{1}{\sqrt{(\bar{k} - \bar{\omega}^2)^2 + 4\zeta^2 \bar{c}^2 \bar{\omega}^2}}, \tag{29}$$

where U represents the displacement amplitude of the mass. Defining the following non-dimensional parameters:

$$\begin{aligned} &\bar{\omega} = \frac{\omega}{\omega_0}, \quad \omega_0 = \sqrt{k/M}, \quad \zeta = \frac{c}{2M\omega_0}, \\ &\bar{k} = \frac{\tilde{k}}{k} = 1 + \frac{\bar{k}_1 \bar{g}_d}{\bar{k}_1 + \bar{g}_d}, \quad \bar{c} = \frac{\tilde{c}}{c} = 1 + \frac{\bar{c}_1 \bar{g}_v}{\bar{c}_1 + \bar{g}_v}, \\ &\bar{k}_1 = \frac{k_1}{k}, \quad \bar{g}_d = \frac{g_d}{k}, \quad \bar{c}_1 = \frac{c_1}{c}, \quad \bar{g}_v = \frac{g_v}{c}, \end{aligned} \tag{30}$$

we derive the non-dimensional forms of Eqs. (26)–(28) as

$$\bar{k} = \begin{cases} \text{for high stiffness,} & \bar{g}_d \leqslant -\bar{k}_1, \\ \text{forlow stiffness,} & -\frac{\bar{k}_1}{1+\bar{k}_1} < \bar{g}_d < 0, \end{cases} \tag{31}$$

$$\bar{c} = \begin{cases} \text{for high damping,} & \bar{g}_v \leqslant -\bar{c}_1, \\ \text{for low damping,} & -\frac{\bar{c}_1}{1+\bar{c}_1} < \bar{g}_v < 0, \end{cases} \tag{32}$$

$$\bar{\Omega} = \frac{\Omega}{\omega_0} = \sqrt{\bar{k}}. \tag{33}$$

From this information, it is seen that ω_0 and ζ denote the supporting frequency and damping factor of the passive system, and $\bar{c}$ represents the ratio $\bar{\zeta}$ of the modified damping $\tilde{\zeta}$ to the original passive damping ζ. That is

$$\bar{\zeta} = \frac{\tilde{\zeta}}{\zeta} = \frac{\tilde{c}}{2M\omega_0\zeta} = \bar{c}. \tag{34}$$

Fig. 11 shows the effect of the displacement feedback gain $\bar{g}_d$ on the non-dimensional supporting frequency $\bar{\Omega}$. As observed in this figure, a feedback gain $\bar{g}_d$ of value a little less than $-\bar{k}_1 = -0.1$ with $\bar{\Omega} \to \infty$ produces a support of very high frequency whilst a feedback gain $\bar{g}_d$ of value a little larger than $-\bar{k}_1/(1+\bar{k}_1) = -0.1/1.1$ with $\bar{\Omega} = 0$ delivers a support of very low

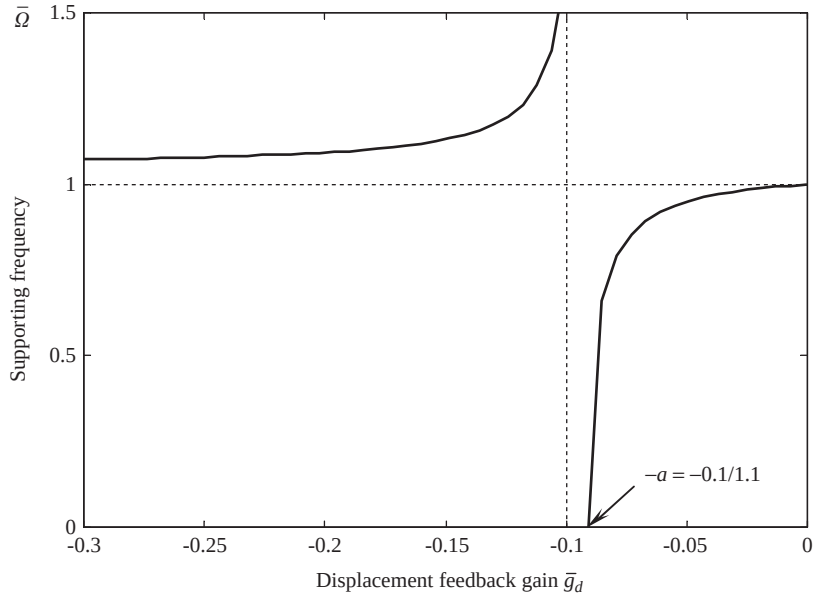

Fig. 11. The effect of the displacement feedback gain $\bar{g}_d$ on the supporting frequency $\bar{\Omega}$.

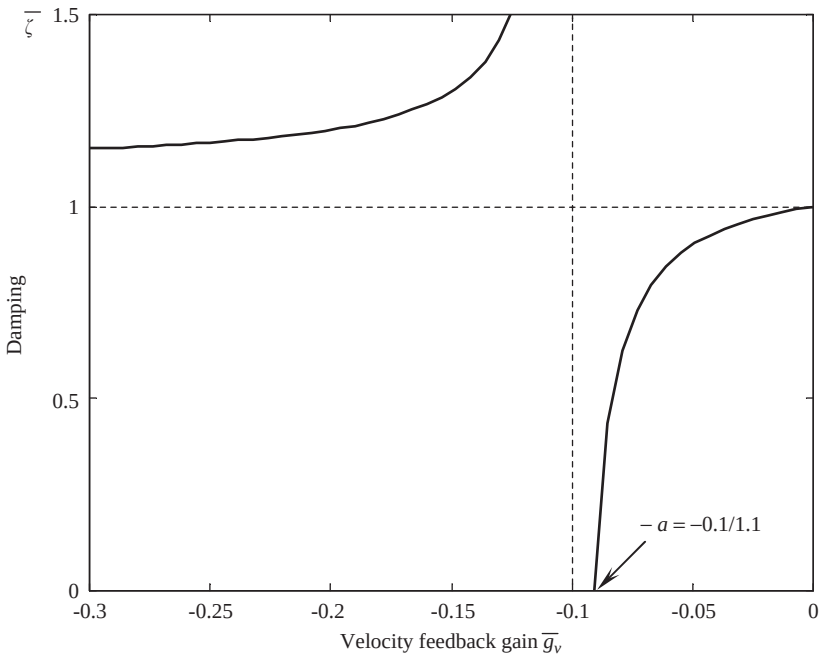

Fig. 12. The effect of the velocity feedback gain $\bar{g}_v$ on damping $\bar{\zeta}$.

frequency. Fig. 12 illustrates the effect of velocity feedback gain $\bar{g}_v$ on the non-dimensional damping $\bar{\zeta}$. It is observed that a feedback gain $\bar{g}_v$ of value a little smaller than $-\bar{c}_1 = -0.1$ with $\bar{\zeta} \to \infty$ provides damping of very high value whereas the feedback gain $\bar{g}_v$ of value a little larger than $-\bar{c}_1/(1+\bar{c}_1) = -0.1/1.1$ with $\bar{\zeta} = 0$ produces a very low damping value. *Due to the fact that parameters $\bar{k}_1$ and $\bar{c}_1$ can be arbitrarily chosen by the designer, the feedback gains $\bar{g}_d$ and $\bar{g}_v$ are therefore practically achievable.*

For the chosen values $\bar{k}_1 = 0.1 = \bar{c}_1$, $\zeta = 0.01$, Figs. 13–15 show the effects of displacement and velocity feedback gains on the displacement response curves. Fig. 13 illustrates the case of different displacement feedback gain values with no velocity feedback control (i.e. $\bar{g}_v = 0$). It is observed that the peaks of the curves with feedback gain values $\bar{g}_d = -0.11, -0.105, -0.101$ (i.e. a little smaller than $-\bar{k}_1 = -0.1$) move towards the right when $\bar{g}_d = 0$, because these chosen feedback gains increase the supporting frequency value. However, the feedback gain values $\bar{g}_d = -(a-0.01), -(a-0.001)$, which are a little larger than the value of $-\bar{k}_1/(1+\bar{k}_1) = -a$, decrease the value of supporting frequencies, so that the peaks move towards the left.

Figs. 14 and 15 show the influence of varying the values of velocity feedback gain on the amplitude factor for displacement feedback gain values $\bar{g}_d = 0$, $-(a-0.001)$, -0.101. It is observed that for a feedback gain $\bar{g}_v$ a little smaller than $-\bar{c}_1 = -0.1$ the amplitude factor decreases because of increasing damping, whereas a feedback gain $\bar{g}_v$ a little larger than $-\bar{c}_1/(1+\bar{c}_1) = -0.1/1.1$ value, the amplitude factor increases because the value of damping decreases.

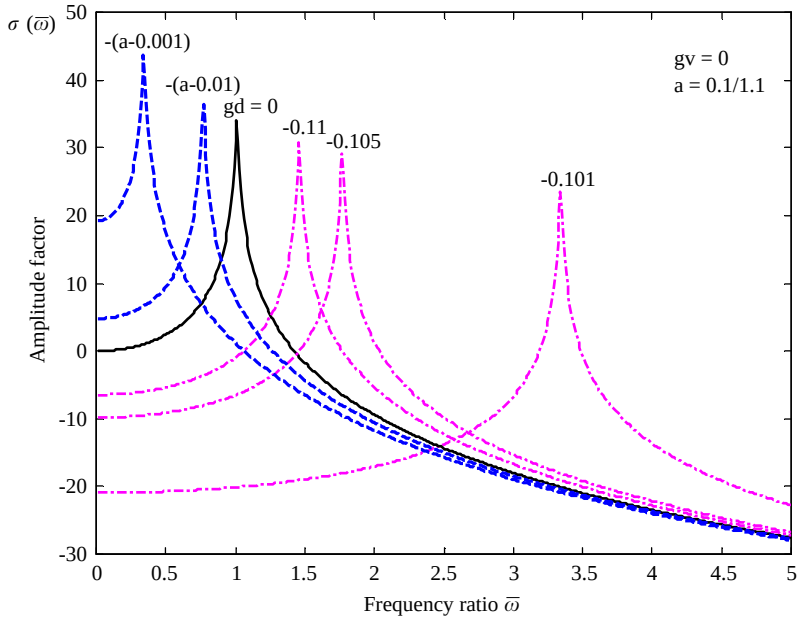

Fig. 13. The displacement frequency response curves affected by the displacement feedback gain $\bar{g}_d(\bar{k}_1 = 0.1 = \bar{c}_1, \zeta = 0.01, \bar{g}_v = 0)$.

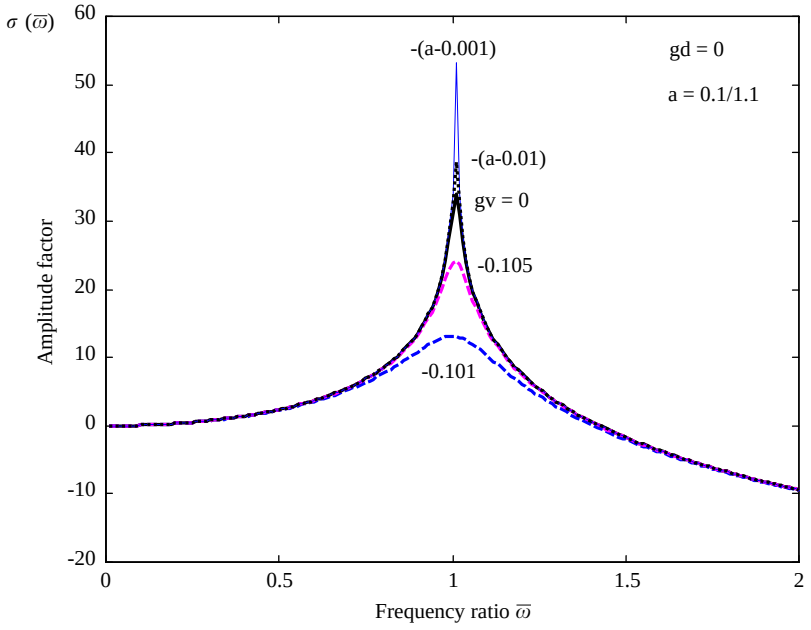

Fig. 14. The displacement frequency response curves affected by the velocity feedback gain $\bar{g}_v(\bar{k}_1 = 0.1 = \bar{c}_1, \zeta = 0.01, \bar{g}_d = 0)$.

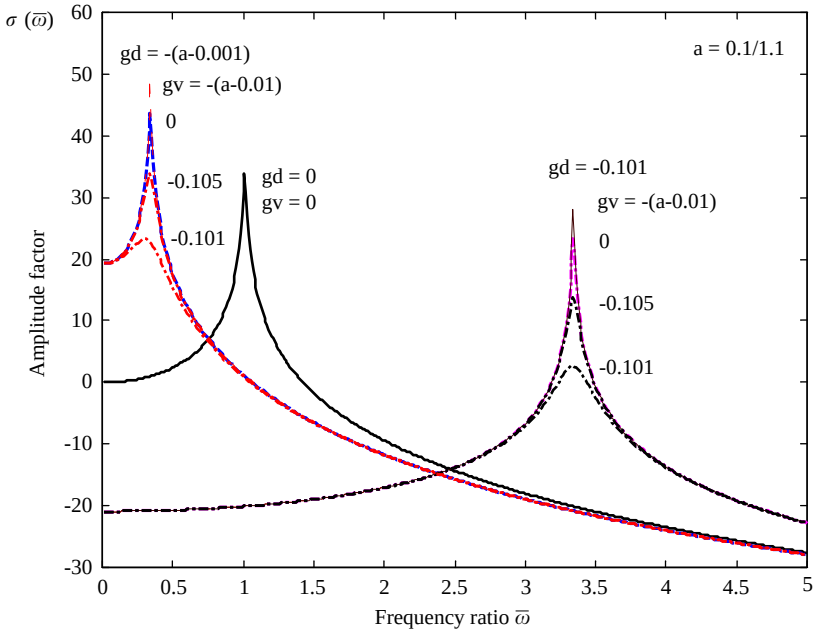

Fig. 15. The displacement frequency response curves affected by the velocity feedback gain $\bar{g}_v(\bar{k}_1 = 0.1 = \bar{c}_1, \zeta = 0.01, \bar{g}_d = -0.101, -(a - 0.001), a = 0.1/1.1)$.

4. Discussion

To achieve a successful isolation system design, many practical problems need be considered. For example, the availability of appropriate actuators, the different types of mechanical springs, sensors, feedback circuit and amplifiers, etc. To design a reliable isolation system for practical use, there is no doubt that validating experiments are necessary. In this present study, only theoretical and conceptual designs are discussed and detail practical problems [3–11] are not pursued. Moreover, the mathematical model and analysis described in this paper are based on the following assumptions: (1) springs, dampers are idealised linear mechanical components such that their mass and nonlinearity are neglected, (2) actuators and the corresponding electrical systems, such as, power amplifiers, sensors, direct current isolators, etc. are idealised components with required frequency characteristics. Applications of this fundamental theory and the theoretical design methods developed allow the assembly of an initial design arrangement. However, in practical systems, these assumptions are not exactly valid. To establish a more accurate model, it is necessary to ease these assumptions and investigate more complex cases (e.g. modelling a continuous actuator as a mass–spring–damper system [13,14], nonlinearity, structure–control interactions influencing characteristics, etc.).

Here, as an example to show a further investigation based on the approach and strategy presented previously, we discuss the effects of the mass m, supporting stiffness K and damping C of a practical actuator, which are neglected in the system shown in Fig. 7. To demonstrate how the generalised feedback control strategies are used to eliminate these effects, the acceleration/velocity feedback gains g_a and g_v are included. Fig. 16(a) shows a practical feedback system using an

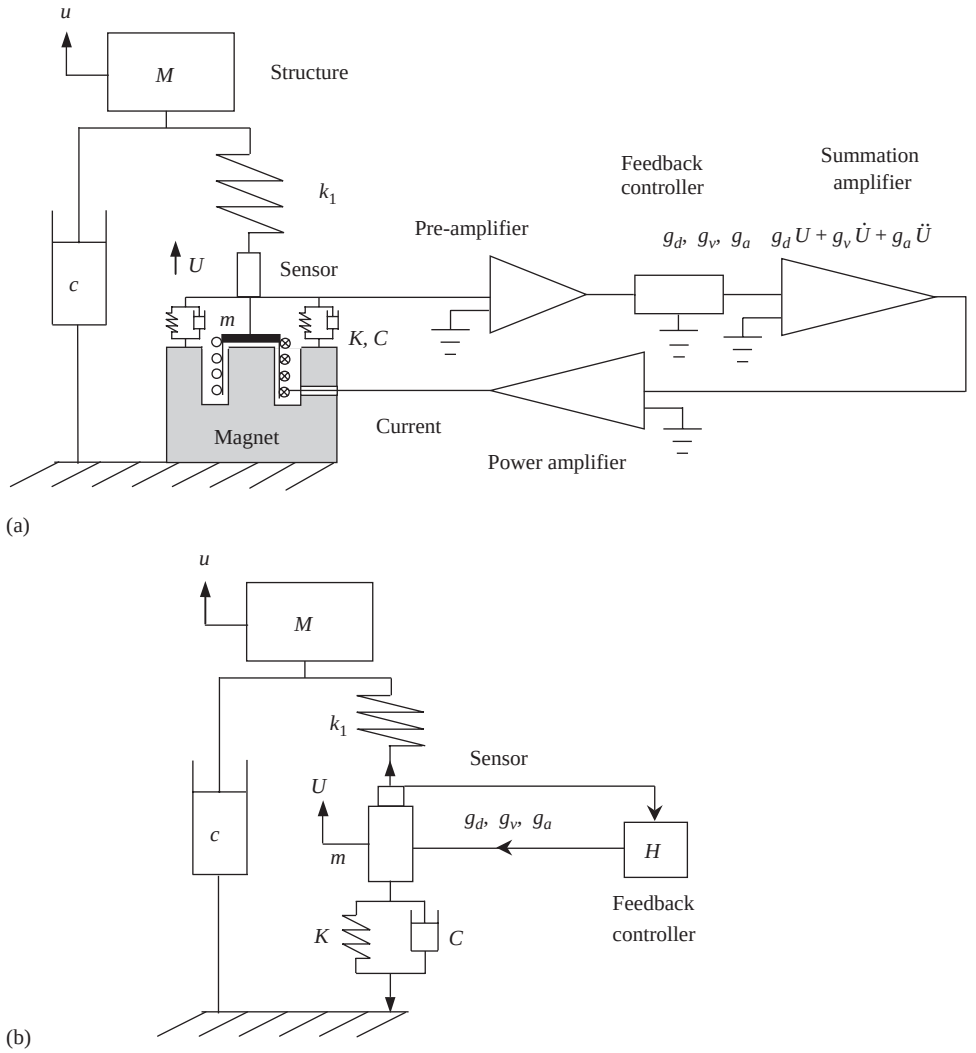

Fig. 16. An active isolation system including a mass–damper–spring unit modelling an practical actuator.

electromagnetic actuator [11]. Here, M represents the mass of a structure, c is the supporting damping coefficient, k_1 is the stiffness of a thin rod connecting the structure and the moving coil of the electromagnetic actuator. The moving parts (coil, sensor, etc.) of the actuator and the sensor have a mass m that is supported by a spring K and a damper C to a magnet fixed on the base. Here, the spring K and the damper C may include other supporting stiffness and damping in parallel with the coil supporting elements, which depends on different requirements of practical applications. The sensor picks up the dynamic signals $U(\dot{U}, \ddot{U})$ of the moving coil. These signals pass through a pre-amplifier, a feedback gains control unit, a summation amplifier and a power amplifier to produce a resultant control current supplied into the moving coil surrounded by the magnetic field to obtain the expected feedback force. This resultant feedback force

consists of three parts involving the displacement, velocity and acceleration feedback, respectively. Fig. 16(b) shows a sketched diagram of the practical system in Fig. 16(a), where the magnet and the three amplifiers are neglected. This system is described by the following equations:

$$\begin{bmatrix} 1 & \\ & \alpha+\tilde{g}_a \end{bmatrix} \begin{bmatrix} \ddot{u} \\ \ddot{U} \end{bmatrix} + 2\zeta\Omega \begin{bmatrix} 1 & \\ & \beta+\tilde{g}_v \end{bmatrix} \begin{bmatrix} \dot{u} \\ \dot{U} \end{bmatrix} + \Omega^2 \begin{bmatrix} 1 & -1 \\ -1 & 1+\gamma+\tilde{g}_d \end{bmatrix} \begin{bmatrix} u \\ U \end{bmatrix} = 0, \tag{35}$$

where $\alpha = m/M$, $\beta = C/c$ and $\gamma = K/k_1$ denote the mass, damping and stiffness ratios, respectively. Other parameters are defined by $\tilde{g}_a = g_a/M$, $\tilde{g}_v = g_v/c$, $\tilde{g}_d = g_d/k_1$, $\zeta = c/2M\Omega$, $\Omega^2 = k_1/M$. The characteristic equation of this system is derived as

$$\begin{aligned}(\alpha+\tilde{g}_a)\lambda^4 + 2\zeta(\alpha+\beta+\tilde{g}_v+\tilde{g}_a)\Omega\lambda^3 + [\alpha+4(\beta+\tilde{g}_v)\zeta^2+\tilde{g}_a+1+\gamma+\tilde{g}_d]\Omega^2\lambda^2 \\ + 2\zeta(\beta+\tilde{g}_v+1+\gamma+\tilde{g}_d)\Omega^3\lambda + (\gamma+\tilde{g}_d)\Omega^4 = 0.\end{aligned} \tag{36}$$

From this equation, the effects of the mass, stiffness and damping of the actuator are discussed as follows:

Case 1: In this example, let us neglect the mass, stiffness and damping of the actuator ($\alpha = \beta = \gamma = 0$). The acceleration feedback gain $\tilde{g}_a$ and the velocity feedback gain $\tilde{g}_v$ can be set to zero and Eq. (36) reduces to

$$(1+\tilde{g}_d)\lambda^2 + 2\zeta(1+\tilde{g}_d)\Omega\lambda + \tilde{g}_d\Omega^2 = 0, \tag{37}$$

which corresponds to the system described in Eq. (17) and schematically visualised in Fig. 7. As discussed in Section 3.2, a suitable chosen feedback gain satisfying $1+\tilde{g}_d \leqslant 0$ provides the required stable, isolation system.

Case 2: Let us now retain the effect of the stiffness of the actuator ($\alpha = 0 = \beta, \gamma \neq 0$). In this example, the acceleration and velocity feedbacks are not needed ($\tilde{g}_a = 0 = \tilde{g}_v$) and Eq. (36) reduces to

$$(1+\gamma+\tilde{g}_d)\Omega^2\lambda^2 + 2\zeta(1+\gamma+\tilde{g}_d)\Omega^3\lambda + (\gamma+\tilde{g}_d)\Omega^4 = 0, \tag{38}$$

which has similar characteristics as Eq. (37). The stiffness of the actuator increases the stiffness of the isolation system designed in Section 3.2. Therefore, the feedback gain $\tilde{g}_d$ satisfying $1+\gamma+\tilde{g}_d \leqslant 0$ is needed to provide the required stable, isolation system.

Case 3: This case studies the effect of the damping of the actuator ($\alpha = 0 = \gamma, \beta \neq 0$). Again, the acceleration feedback is not needed, i.e. $\tilde{g}_a = 0$ and Eq. (36) reduces to

$$2\zeta(\beta+\tilde{g}_v)\lambda^3 + [4(\beta+\tilde{g}_v)\zeta^2+1+\tilde{g}_d]\Omega\lambda^2 + 2\zeta(\beta+\tilde{g}_v+1+\tilde{g}_d)\Omega^2\lambda + \tilde{g}_d\Omega^3 = 0. \tag{39}$$

To eliminate the effect of damping in the actuator, a negative velocity feedback $\tilde{g}_v = -\beta$ is chosen to reduce Eqs. (39)–(37) and therefore satisfies the original design requirement. To avoid non-stability of the system caused by the operational error of $\tilde{g}_v + \beta \approx 0$, a little lower velocity feedback gain

$$\tilde{g}_v < -\beta \tag{40}$$

is chosen which in association with condition $1+\tilde{g}_d \leqslant 0$ is required for the stability of solution of Eq. (39).

Case 4: This example investigates the effect of the mass of the actuator ($\beta = \gamma = 0, \alpha \neq 0$). Here, the velocity feedback is not needed, i.e. $\tilde{g}_v = 0$ and Eq. (36) reduces to

$$(\alpha + \tilde{g}_a)\lambda^4 + 2\zeta(\alpha + \tilde{g}_a)\Omega\lambda^3 + [\alpha + \tilde{g}_a + 1 + \tilde{g}_d]\Omega^2\lambda^2 + 2\zeta(1 + \tilde{g}_d)\Omega^3\lambda + \tilde{g}_d\Omega^4 = 0. \quad (41)$$

To eliminate the mass effect of the actuator, a negative acceleration feedback $\tilde{g}_a = -\alpha$ is required in order to reduce Eqs. (41)–(37) and therefore satisfies the original design requirement. However, the operational error of $\tilde{g}_a + \alpha \approx 0$ may cause instability in the system in practical situations, because the stability condition of Eq. (41) requires that

$$\tilde{g}_a + \alpha > 0, \quad \tilde{g}_d > 0. \quad (42)$$

However, because stiffness and damping of the actuator are neglected in this example, this unstable practical situation can be avoided as described by the procedure discussed in the following case.

Case 5: To complete this investigation, the effects of mass, stiffness and damping of the actuator are all considered. In this general case, three feedback control strategies are adopted. The velocity and acceleration feedback gains can be chosen to satisfy $\tilde{g}_v = -\beta$ and $\tilde{g}_a = -\alpha$ to eliminate their effect and this substitution reduces Eqs. (36)–(38) thus satisfying the design requirement. To guarantee the stability of the system described in Eq. (36), it is required to choose values for both velocity and acceleration feedback gains a little lower than their respective idealised values ($\tilde{g}_v = -\beta$ and $\tilde{g}_a = -\alpha$). That is

$$\tilde{g}_v < -\beta, \quad \tilde{g}_a < -\alpha, \quad 1 + \gamma + \tilde{g}_d \leqslant 0. \quad (43)$$

This equation indicates that the feedback system realises some forces having the characteristics of a negative mass, damping or stiffness, respectively, in the total mechanical-control system. This concept has been widely used in vibration tests to measure the natural characteristics of a system using the called *electrical stiffness/mass technique* [11].

Fig. 17(a–c) shows the effects of mass α, damping β and stiffness γ of the actuator on the displacement amplifying factor of the supporting system in comparison to the original design shown in Fig. 7. The original system is designed based on an idealised actuator ($\alpha = \beta = \gamma = 0$) and a negative displacement feedback gain $\tilde{g}_d = -1.01$ to obtain a higher supporting stiffness. It is found that inclusion of the mass α of the actuator decreases the supporting frequency as shown in Fig. 17(a) and the additional damping β increases the damping and reduces the displacement amplifying factor shown in Fig. 17(b). The additional stiffness γ, satisfying $1 + \gamma + \tilde{g}_d \leqslant 0$, increases the supporting frequency of the system as shown in Fig. 17(c). However, inclusion of a higher additional stiffness γ value (e.g. $\gamma = 0.05$) causes $1 + \gamma + \tilde{g}_d > 0$ and as shown in Fig. 17(c) decreases the supporting frequency magnitude significantly. Therefore, to use a higher additional stiffness value γ it is necessary to decrease the negative displacement feedback gain $\tilde{g}_d$ to satisfy the condition $1 + \gamma + \tilde{g}_d \leqslant 0$.

Fig. 18 shows how to use the acceleration, velocity and displacement feedback control strategies studied herein to cancel the effects of the additional mass α, damping β and stiffness γ of a practical actuator on the dynamic characteristics of the supporting system. In this figure, curve 1 corresponds to the case of an idealised actuator ($\alpha = \beta = \gamma = 0$) designed in Fig. 7 ($\tilde{g}_a = 0, \tilde{g}_v = 0, \tilde{g}_d = -1.01$). Curve 2 shows the dynamic characteristics of a supporting system affected by the additional mass $\alpha = 0.01$, damping $\beta = 0.01$ and stiffness $\gamma = 0.01$ of a practical actuator. Because

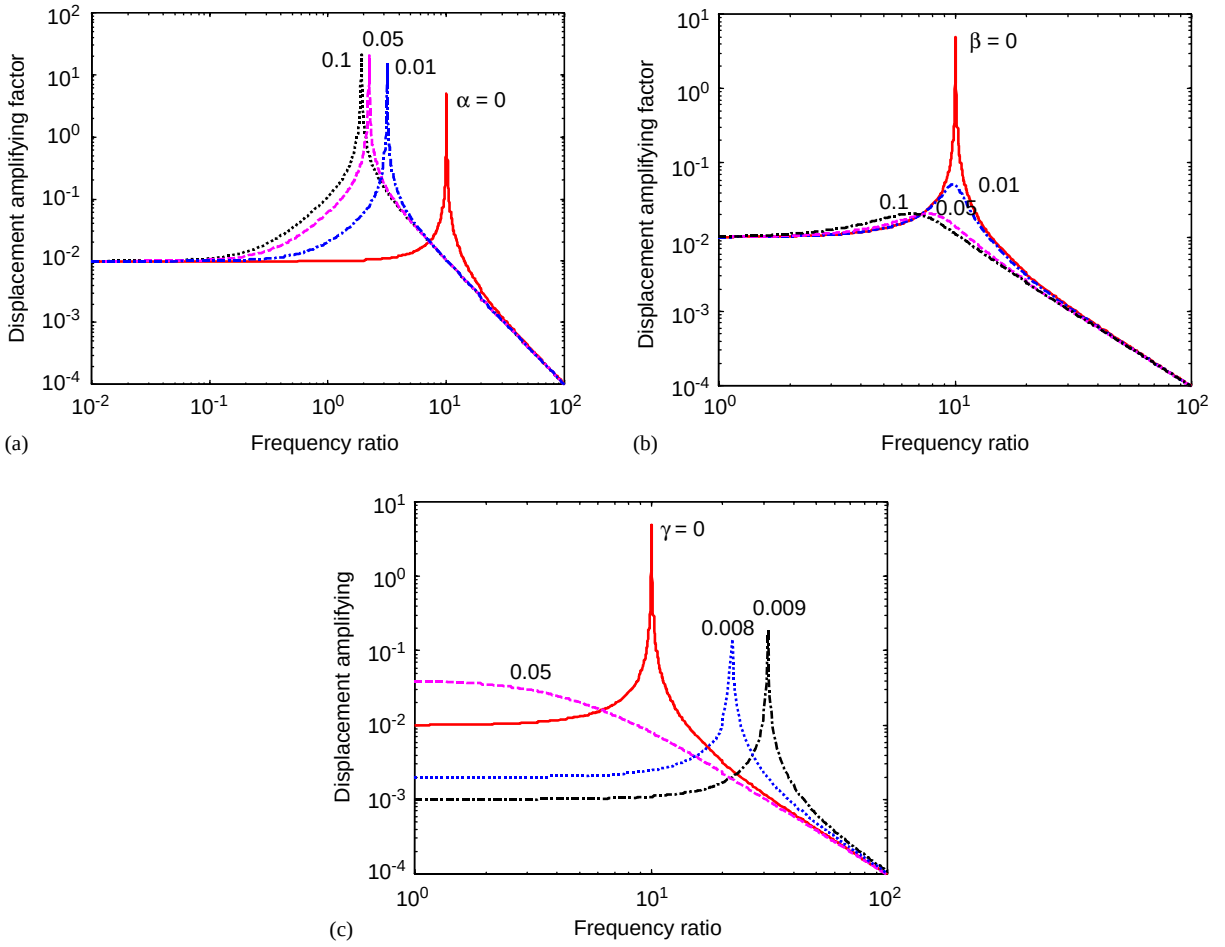

Fig. 17. The effects of mass α, damping β and stiffness γ of the actuator on the displacement amplifying factor of the isolation system shown in Fig. 7 ($\tilde{g}_a = 0, \tilde{g}_v = 0, \tilde{g}_d = -1.01$).

of the effects of the additional mass, damping and stiffness, the whole system becomes a system of two degrees of freedom and there appears an additional lower natural frequency, which significantly reduces the dynamic supporting stiffness. To eliminate these effects, the feedback control gains $\tilde{g}_a = -\alpha$, $\tilde{g}_v = -\beta$ and $\tilde{g}_d = -1.01 - \gamma$ are chosen, which exactly produces a curve similar to curve 1. To avoid an unstable possibility caused by any operational error as described previously, the feedback gains $\tilde{g}_a = -\alpha - 0.001$ and $\tilde{g}_v = -\beta - 0.001$ are chosen to satisfy the stability conditions given in Eq. (43). The dynamic characteristics associated with this set of feedback gain values is described by curve 3 in Fig. 18. It is observed that there exists an anti-resonance peak in the curve, which does not reduce the designed dynamic supporting stiffness but provides an improved control effect.

For the system considered in this study, such as the system illustrated in Fig. 9, similar discussions can be undertaken to include the effects of mass, stiffness and damping of a practical actuator.

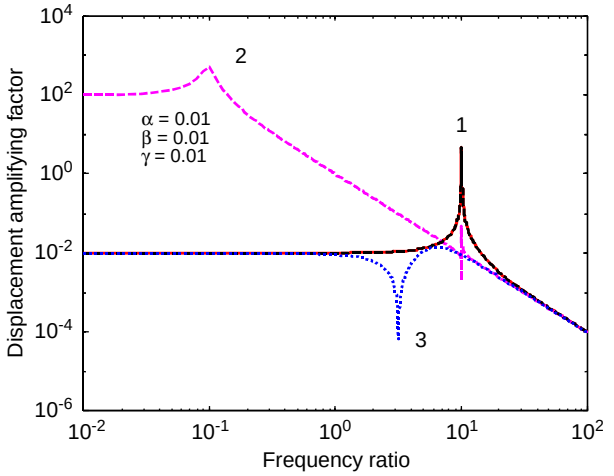

Fig. 18. Acceleration, velocity and displacement feedback control values are used to cancel the effects of additional mass α, damping β and stiffness γ of a practical actuator on the displacement amplifying factor of the isolation system shown in Fig. 7.

In this investigation, constant feedback gains are adopted for displacement, velocity and acceleration controls. Such measures are convenient in the practical design of feedback systems involving electrical and mechanical units. Alternatively, a frequency-dependent feedback gain may be used to eliminate the effects of mass, damping and stiffness, but this lies outside the scope of the present study.

5. Conclusion

The generalised theory described herein includes acceleration feedback controls, which produce a negative effect on the value of the natural frequency, compared with displacement feedback controls. In general, a negative displacement feedback gain decreases the stiffness of the system and a positive acceleration feedback gain increases inertia, and therefore both of these feedback controls decrease the natural frequency of the system. To determine the influence of the supporting system on the natural dynamic characteristics of the structure in mode experiments, the most important parameter is the frequency of the supporting system, which is dependent on both stiffness and mass influences. This study provides no examples illustrating acceleration feedback control, although through development of the mathematical model this may be used to adjust only the effective mass of the system.

It has been demonstrated that the original study [5,6] involving parallel and series connections of an active spring with a mechanical spring to produce an infinite or zero value of the supporting stiffness has been extended to more generalised cases by examining the influence of dynamic modulus involving active–passive stiffness, damping and inertia forces. This extension provides a theoretical basis to design an isolation system with infinite or zero modulus through the introduction of infinite or zero stiffness and/or damping as described. To avoid the limitations of

feedback gain in practical designs, it is shown that a mixture of parallel and series connected passive systems with active actuators can produce benefits. These new suspension systems use limited feedback gains of achievable magnitude to produce a very low natural frequency support, a significantly large stiffness support, a significantly large value of damping or a self-excited vibration oscillator with zero damping. The proposed and developed design philosophy may be applied to design suspension systems to meet prescribed specified requirements. For example, a combination of the proposed systems shown in Figs. 6 and 9 provides the comprehensive isolation system shown in Fig. 10. This system has adjustable (i.e. low or high) values of frequency and damping of the support using both displacement and velocity feed back controls. The displacement frequency response curves for this system provide understanding of the control mechanism. By extending the approach developed herein, various hybrid vibration control systems with increased control performance can be designed for practical applications.

References

[1] C.M. Harris, C.E. Crede, *Shock and Vibration Handbook*, second ed., McGraw-Hill, New York, 1976.
[2] W.T. Thomson, *Theory of Vibration with Applications*, third ed., Prentice-Hall, London, 1988.
[3] G. Nakhaie Jazar, F. Golnaraghi, Engine mounts for automotive applications: a survey, *Shock and Vibration Digest* 34 (5) (2002) 363–379.
[4] R.G. Cobb, J.M. Sullivan, A. Das, L. Porter Davis, T. Tupper Hyde, T. Davis, Z.H. Rahman, J.T. Spanos, Vibration isolation and suspension system for precision payloads in space, *Smart Materials & Structures* 8 (6) (1999) 798–812.
[5] D.L. Platus, Negative-stiffness-mechanism vibration isolation systems, in: E.A. Derby, et al. (Eds.), *Proceedings of SPIE Conference on Current Developments in Vibration Control for Optomechanical Systems*, SPIE, vol. 3786, 1999, pp. 98–105.
[6] T. Mizuno, Vibration isolation system using zero-power magnetic suspension, *Proceedings of 15th IFAC World Congress (CD-ROM)* 955 (2002) 1–6.
[7] T. Mizuno, Y. Takamori, A transfer-function approach to the analysis and design of zero-power controllers for magnetic suspension systems, *Electrical Engineering in Japan* 141 (2002) 67–75.
[8] T. Mizuno, H. Suzuki, Y. Takamori, Development of an active vibration isolation system using zero-power magnetic suspension. *Proceedings of Tenth International Congress on Sound & Vibration (CD-ROM), IISV*, 2003, pp. 887–894.
[9] M.K. Kwak, M.H. Kwak, S. Heo, Development of the passive–active vibration absorber using piezoelectric actuators, *Proceedings of SPIE—The International Society for Optical Engineering* 4697 (2002) 292–300.
[10] C.R. Fuller, S.J. Elliott, P.A. Nelson, *Active Control of Vibration*, Academic Press, San Diego, 1996.
[11] J.T. Xing, *Theory and Techniques on Mode Vibration Experiments of Aircraft Structures, Lecture Notes*, NAI Press, Nanjing, China, 1975 (in Chinese).
[12] R. Yorke, *Electric Circuit Theory*, Pergamon, Oxford, 1981.
[13] S.J. Elliott, L. Benassi, M.J. Brennan, P. Gardonio, X. Huang, Mobility analysis of active isolation systems, *Journal of Sound and Vibration* 271 (2004) 297–321.
[14] L. Benassi, S.J. Elliott, P. Gardonio, Active vibration isolation using an inertial actuator with local force feedback control, *Journal of Sound and Vibration* 278 (2004) 705–724.